



# Correlating and evaluating the functionality-related properties with surface texture parameters and specific characteristics of machined components

Quanren Zeng\*, Yi Qin\*, Wenlong Chang, Xichun Luo

Centre for Precision Manufacturing, Department of Design, Manufacture and Engineering Management, University of Strathclyde, G1 1XQ Glasgow, UK

## ARTICLE INFO

### Keywords:

Surface texture  
Functionality-related properties  
Grinding  
Ni-based superalloy  
Machinability

## ABSTRACT

Machining-process-induced surface texture plays an indispensable role in determining surface integrity and final functional performance of the machined components. Although there are already many existing standard parameters for quantitatively characterizing the machined surface, accurately describing and effectively correlating the 3D surface texture parameters and specific characteristics with the relevant functional performances in practice, are still not well solved. The inadequacy of using 2D single-valued surface profile parameters and the non-ubiquity of using 3D areal surface texture parameters in industry are the main obstacles. The research reported in this paper addressed this issue by proposing a practical means which makes use of both 3D surface texture parameters and statistical functions for surface geometrical characterization and functional correlation and evaluation. To better investigate the influence of machining-induced surface texture and its characterization on the functionality-related performance of machined surfaces, Ni-based superalloy GH4169, a typical difficult-to-machine material widely used in aircraft industry, was selected for the machining experiment. Two kinds of mechanically-processed surfaces, one ground and the other turned, both having an identical value of 3D arithmetic mean deviation ( $S_a$ ), were quantitatively characterized and analyzed using 2D and 3D surface texture parameters. Considering that the measured 3D surface texture is of random nature, the corresponding functionality-related performances were also investigated with statistical functions, e.g. power spectral density (PSD) and auto-covariance (ACV). Correlation between the 3D surface texture parameters or statistical functions with the corresponding functional performance, e.g. contact, running-in wear and lubricant retention, were then established. This study emphasized on the effectiveness and veracity of the 3D surface texture parameters and statistical functions in characterizing and evaluating machined-surface performance along with the traditional 2D parameters. It is especially suitable for machining materials whose functionality-related properties are machining-process-sensitive and surface-texture-dependent.

## 1. Introduction

The machining-induced surface texture strongly influences the mechanical properties and functional performance of the machined components or products, such as tribologically-related properties [1,2], load-bearing capability [3,4], fatigue properties [5], optical properties [6], abrasion and corrosion resistance, as well as the aesthetic appearance desired by customers. Simply, surface texture could be defined as the repetitive or random deviations from a nominal surface which in reality form a three-dimensional (3D) topography. Sometimes, it is also used interchangeably with surface topography in the manufacturing and machining fields [7]. Generally speaking, characterization of surface texture involves at least 2 aspects: (1) defining accurate parameters to quantify the surface micro geometrical features and (2) selecting reasonable parameters to adequately describe and evaluate the corre-

sponding functional properties of surface [8]. The ever-increasing demand for high-quality and high-precision engineering components operating under some extreme working conditions, requires the use of high-performance materials and the high-accuracy characterization as well as effective correlation of the machining-induced surface texture with relevant functional performance [9–11]. In order to improve the capability of accurately characterizing and evaluating the functional performance of a machined surface, it would be helpful to have well-defined 2D or 3D surface texture parameters (e.g.  $R_a$  or  $S_a$ ). Once surface micro geometrical features and functionality-related characteristics are quantitatively characterized by corresponding texture parameters, the functional performance of machined surfaces could be correlated and predicted. With this, corresponding machining conditions could also be adjusted accordingly to guide the production of surfaces with desirable geometrical features and functional performances [12,13].

\* Corresponding authors.

E-mail addresses: [quanren.zeng@strath.ac.uk](mailto:quanren.zeng@strath.ac.uk) (Q. Zeng), [qin.yi@strath.ac.uk](mailto:qin.yi@strath.ac.uk) (Y. Qin).

Normally, a specific machining process corresponds to a specific geometrical feature or functional property on the machined surface of the mechanical component. There are many different ways to describe and quantify the surface micro geometrical features of a machined component. The most widely accepted and used are the conventional 2D surface profile parameters which are considered as the primary indexes for surface characterization and quality assessment in the manufacturing practice. However, the 2D characterization approach does not accommodate the 3D nature of surfaces; although many researchers have tried to correlate 2D surface profile parameters with specific functionality-related properties, there is a consensus that using standard 2D surface profile parameters alone is inadequate for comprehensively describing and characterizing surface functionalities. Developments in computer technology have led to the realization of improved methods for measuring and characterizing the surfaces of machined components [14,15]. Current 3D surface texture measurement and characterization techniques have the capability to take into account the anisotropy of surfaces and provide a more in-depth understanding of the correlation between surface texture and its corresponding functional performance. However, there are already many 3D surface texture characteristic parameters and they are too complicated to be comprehended and implemented all at once. Hence, selecting relevant, requisite and reasonable 3D surface texture parameters for quantitative description and characterization of the machined surface is critical for the prediction and evaluation of corresponding machined surface functionalities, such as friction, lubricant retention, abrasion resistance, bearing loading and even fatigue properties [8,16].

To investigate how the surface texture parameters and specific characteristics could be better correlated with the functionality-related performance of the machined surfaces, a typical difficult-to-machine Ni-based superalloy GH4169 which is widely used in aircraft manufacturing, is selected in this paper for the cutting test and subsequent surface characterization analysis. Grinding and turning processes are carried out and the principal 3D surface texture parameters (such as  $S_a$ ,  $S_{ci}$ ,  $S_{vi}$ ,  $S_{al}$ ,  $S_{dr}$ ) are measured for quantitatively characterizing the surface topography and relevant functionalities of the ground and turned surfaces. Further, considering the measured 3D surface textures are of random nature, the corresponding functionality-related performances are also investigated and discussed with statistical functions, such as power spectral density (PSD) and auto-covariance (ACV). The correlation between machined surface texture characteristics and functionality-related properties (e.g. surface contact, running-in wear and lubricant retention), are also discussed by comparing and analyzing the measured 3D surface texture parameters and statistical functions of the two surfaces.

## 2. 2D and 3D surface characterization parameters

Real surfaces of machined components are not completely smooth. They are essentially composed of many microscopic irregular peaks and valleys from the microscopic point of view. All of these asperities combined constitute the surface texture of machined components. It is mainly introduced by various aspects of manufacturing process. The conditions of a machining process affect the characteristics of a surface and machining parameters can be selected to produce particular characteristics. For a 2D surface profile, the surface texture is geometrically a combination of asperities of different wavelengths; the wavelength can be used to classify surface texture into different scales or levels [7,17]. As shown in Fig. 1, according to the difference of height and wavelength, the 2D rough surface can be decomposed into three components: surface roughness, surface waviness and error of form. Surface roughness, commonly referred to as surface finish, is mainly due to the surface friction between the tool and the workpiece, plastic deformation during separation of chips and the tool feed marks. Surface roughness is superimposed on the surface waviness. The wavelength of surface waviness is usually greater than that of surface roughness; it is normally caused by the chatter of the machine tool, and workpiece deflection or vibration.

The error of form represents the deviation between the actual overall shape and the ideal shape of the surface and its wavelength is larger than that of waviness; it may be caused by the inaccuracies of the slide-way in machine tools or the unbalance of grinding wheels. In general, wavelength and height of surface roughness are relatively small. In engineering practice, the wavelength  $\lambda$  of surface roughness is normally considered to be less than 1 mm; the wavelength of surface waviness is usually within the range of 1–10 mm; and the wavelength of error of form is usually greater than 10 mm. For 2D representation, it is conventional to define surface texture as a combination of surface roughness and waviness only. In this research, the focus is on the functional effect of surface topography characterization and the terms surface roughness and surface texture are regarded as synonymous in the 2D situation.

### 2.1. 2D surface profile parameters

The purpose of surface texture characterization is to give an accurate representation of all micro geometrical features and to describe them as precisely as possible. Many techniques, such as virtual visual characterization, meet the purpose of surface characterization [18,19]. However, the most convenient approach in practice, is to describe a surface by a set of roughness parameters which can be objectively measured and accurately related to the functional properties of machined surfaces. There is a great variety of surface roughness parameters, many of which have been developed to describe geometrical features or characterize the functionalities of surfaces for particular applications [20–24]. All the time the most commonly-used single-value parameters for characterizing and assessing the surface texture and quality of machined components are the average roughness ( $R_a$ ) and the root-mean-square roughness ( $R_q$ ).  $R_a$  describes the arithmetical average deviation of surface height from the mean line within the sampling length  $L$ . It is widely used in the automotive and metalworking industries to specify the surface roughness of various components ranging from cylinder bores to brake drums.  $R_q$  evaluates the root-mean-square value of surface height within a sampling length. It is generally more sensitive to peaks and valleys than  $R_a$  and is commonly specified for surfaces of optical components. In addition to these 2 average height parameters, some extreme height parameters have also been defined for different applications. For example,  $R_t$  represents the height from the maximum peak to the lowest valley within an evaluation length. It is sensitive to large deviations from the mean line or scratches on the surface and is widely used along with  $R_a$  to describe and characterize surface profiles of machined components. The continuum and discrete forms for  $R_a$ ,  $R_q$  and  $R_t$  are listed in the Table 1.

To better correlate and evaluate surface geometrical characteristics with practical functionalities of machined components, shape distribution parameters, skewness  $R_{sk}$  and kurtosis  $R_{ku}$ , are also introduced as shown in Table 1.  $R_{sk}$  is defined as the skewness of the surface profile to be assessed and it is a measure of the asymmetry of the profile about its mean line. Negative  $R_{sk}$  indicates a predominance of sharp valleys and rounded peaks, whilst positive  $R_{sk}$  means a surface with more round valleys and sharp peaks, as shown in Fig. 2(a). Material removal processes such as grinding, honing and milling are likely to produce negatively skewed surfaces which are usually good for load bearing and oil retention properties; while processes such as sandblasting, EDM and turning are apt to produce positively skewed surfaces which can provide good gripping or locking ability. If the extremes of a profile are symmetrically distributed with respect to both sides of the mean line,  $R_{sk}$  will be zero.  $R_{ku}$  is defined as the kurtosis of the surface profile to be assessed and is a measure of the degree of peakedness. As shown in Fig. 2(b), if  $R_{ku} > 3$  it is normally called leptokurtic and the surface profile has many high peaks or deep valleys. If the  $R_{ku} < 3$ , it is normally called platykurtic and means the surface profile has relatively few high peaks and low valleys. For a surface profile of Gaussian distributions,  $R_{ku} = 3$ .

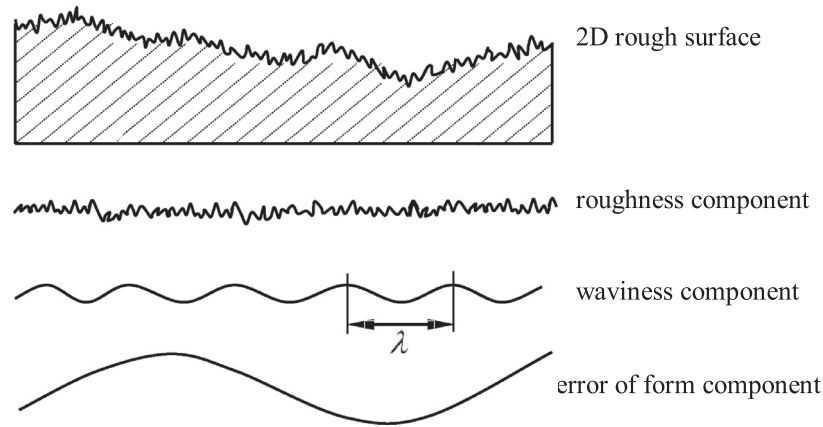


Fig. 1. Schematic diagram of the basic components of a 2D rough surface.

Table 1

Typical and common-used 2D surface profile parameters [9, 20].

2D surface profile parameters		Continuum or discrete forms
$R_a$	Profile average roughness	$R_a = \frac{1}{L} \int_0^L  z(x)  dx = \frac{1}{n} \sum_{i=1}^n  z(x_i) $
$R_q$	Root-mean-square roughness	$R_q = \sqrt{\frac{1}{L} \int_0^L [z(x)]^2 dx} = \sqrt{\frac{1}{n} \sum_{i=1}^n z(x_i)^2}$
$R_t$	Maximum peak-to-valley height	$R_t = z(x_i)_{max} - z(x_i)_{min}$
$R_{sk}$	Skewness of profile height distribution	$R_{sk} = \frac{1}{R_q^3} \left[ \frac{1}{L} \int_0^L z(x)^3 dx \right] = \frac{1}{R_q^3} \left[ \frac{1}{n} \sum_{i=1}^n z(x_i)^3 \right]$
$R_{ku}$	Kurtosis of profile height distribution	$R_{ku} = \frac{1}{R_q^4} \left[ \frac{1}{L} \int_0^L z(x)^4 dx \right] = \frac{1}{R_q^4} \left[ \frac{1}{n} \sum_{i=1}^n z(x_i)^4 \right]$

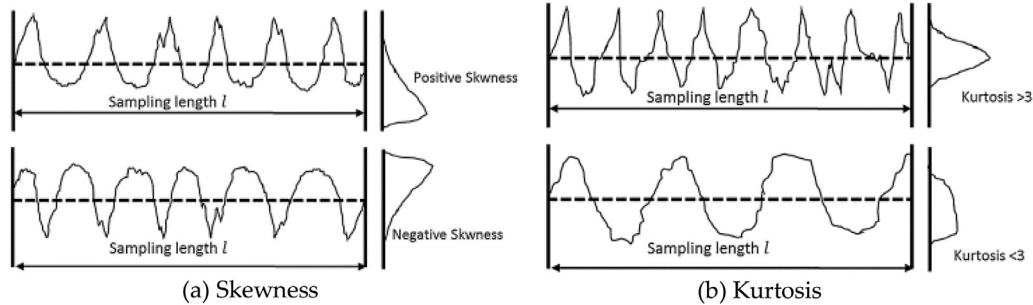


Fig. 2. Definitions of 2D surface roughness parameters: (a) skewness and (b) kurtosis [25,26].

## 2.2. Statistical functions

The surface texture of a machined component is complex and with random irregularities at the microscopic scale, e.g. the machined surface by grinding is of random and statistical information by nature. Accurate characterization of the wide variety of surface texture produced by various machining processes requires more than one of the above-mentioned single-value statistical parameters; certain statistical functions formulated for random process theory and time series analysis can enable more detailed characterization to be achieved. Many statistical functions have been developed to characterize random surface profiles [9,20], and the most commonly-used are the amplitude distribution function (ADF), bearing area curve (BAC), power spectral density (PSD) function and auto-covariance (ACV) function. A comprehensive understanding of their definitions and relationships is absolutely necessary prior to accurately characterizing and assessing surface texture features and functionalities.

The amplitude distribution function (ADF), sometimes also as the probability density distribution or histogram, describes the probability density of surface height; its plot shows the distribution of the number of points along different surface heights [9,20]. The bearing area

curve (BAC), also called as the Abbott-Firestone curve or bearing ratio curve, is defined as the ratios of a length obtained by intersecting a line at different heights to the profile. Statistically, the BAC could be obtained by integrating the surface profile trace. Fig. 3 shows the correlation between a surface profile and its ADF and BAC. The BAC is one of the most important characterization methods in surface profilometry for the assessment of lubricant retention properties, wear resistance and load-bearing capacity; it is particularly suitable for characterizing surfaces which are flat on the top and grooved or notched at the bottom. Normally, five surface characterization parameters,  $R_{pk}$ ,  $R_k$ ,  $R_{vk}$ ,  $M_{r1}$  and  $M_{r2}$ , as shown in Table 2, are defined within the BAC. The method of how to derive these parameters is shown in Fig. 4 and is based on a best-fit line over 40% of the BAC central portion [20,27].

Further, considering that some machined surface features are of random nature, they can conveniently be characterized using statistical functions such as power spectral density (PSD) and auto-covariance (ACV). PSD analysis is useful for studying the weights of various periodic components in a surface profile. It decomposes the measured surface texture geometry into different components of spatial frequencies using Fourier transforms and provides more information than single-value parameter  $R_a$  or  $R_t$  does. Mathematically, the PSD is defined as

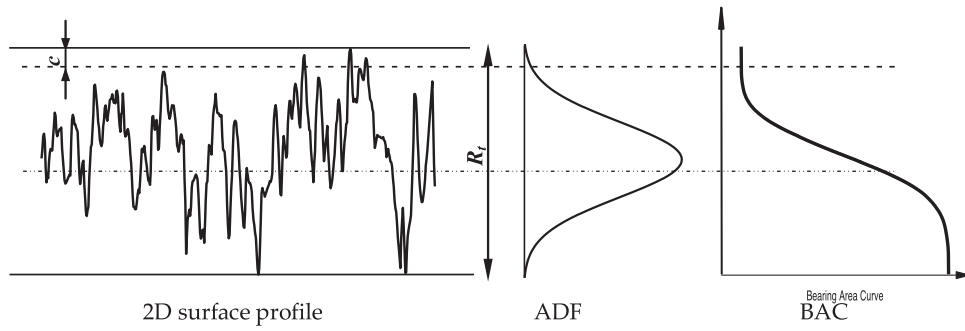


Fig. 3. Externally-ground 2D surface profile and corresponding ADF and BAC.

Table 2

Typical BAC-related surface roughness parameters [20,24,25].

2D BAC parameters	Definition or description
$R_{pk}$	Reduced peak height
$R_k$	Core roughness depth
$R_{vk}$	Reduced valley depth
$M_{r1}$	Peak material portions
$M_{r2}$	Valley material portions

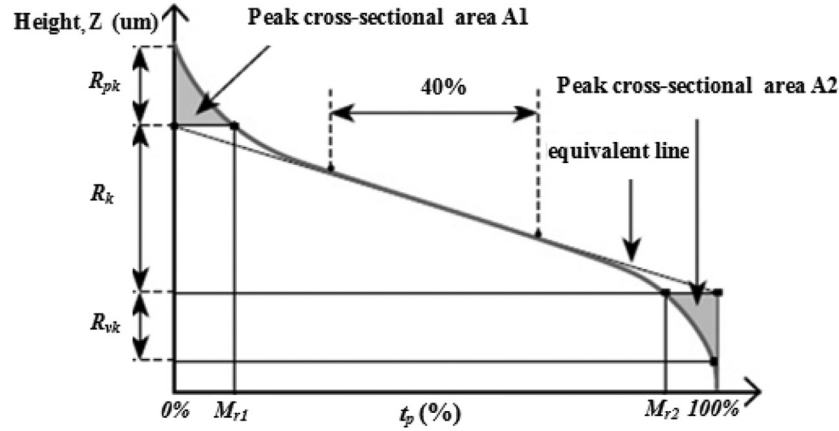


Fig. 4. BAC and related surface parameters with respect to functionality [27].

the square of the Fourier transform of the measured surface texture and it can be expressed as [9,23]:

$$\text{PSD}(f) = \frac{d_0}{N} \left| \sum_{j=1}^N Z_j \cdot \exp[-i \cdot 2\pi f(j-1)d_0] \right|^2 \quad (1)$$

where  $i = \sqrt{-1}$ ;  $d_0$  is the sampling length;  $Z_j$  is the surface amplitude function; the spatial frequency  $f$  equal to  $K/L$ , where  $K$  is an integer that ranges from 1 to  $N/2$ ;  $N$  is the number of sampling points.

The ACV is defined as the covariance of the variables against a translated surface profile of itself and indicates how well the shifted surface profile correlates with the original one and gives a measure of the randomness of the surface. For 2D surface profile analysis, ACV is the inverse Fourier transform of the PSD. The magnitude of ACV is a measure of how similar the surface profile or texture is at a given distance from another location. If the shifted version of the surface is similar or identical to the other surface, then its value of ACV stays near unity for a given distance. If the shifted surface is such that all peaks align with the corresponding valleys of the original one, then its value of ACV approaches  $-1$ . When the ACV falls rapidly to zero along a given direction, the shifted surface profile is different and thus ‘uncorrelated’ with the surface at the original measurement location.

### 2.3. 3D surface texture parameters

With the development of measurement techniques and equipment, 3D characterization method and 3D surface texture parameters have been invented to exhibit and analyze more complete and integrated surface characterization [18,19]. Visualized analysis of 3D surface texture is also becoming convenient and practical; this therefore leads to the prevalence of producing customized surface texture by controlling reasonable processing parameters.

Generally, some of the commonly-used 2D surface roughness parameters are suitable and easy to be extended to constitute the corresponding 3D surface texture parameters. However, for accurately characterizing some particular functionality-related properties of a machined surface, specifically-designed 3D surface parameters that correlate well with performance are also needed. For several decades, many 3D surface texture characterization parameters have been put forward to quantitatively measure and characterize engineering surfaces and corresponding functional properties. The most renowned and acceptable 3D surface texture parameters are the ‘Birmingham 14’ parameter set [9]. Compared with 2D surface roughness parameters denoted with a letter ‘R’, 3D surface texture parameters all start with a letter ‘S’. For example,  $S_q$ , the root-mean-square deviation of surface, is an extension of 2D surface roughness parameter  $R_q$ ; while  $S_a$ , the arithmetic mean deviation

**Table 3**  
The 3D surface texture parameters [21,22].

3D surface texture parameters		Continuum or discrete forms
$S_q$	Root-mean-square deviation of surface	$S_q = \sqrt{\frac{1}{MN} \sum_{j=1}^N \sum_{i=1}^M [z(x_i, y_j)]^2}$
$S_a$	Arithmetic mean deviation of the surface	$S_a = \frac{1}{MN} \sum_{j=1}^N \sum_{i=1}^M  z(x_i, y_j) $
$S_{sk}$	Skewness of surface texture height distribution	$S_{sk} = \frac{1}{MN S_q^3} \sum_{j=1}^N \sum_{i=1}^M z^3(x_i, y_j)$
$S_{ku}$	Kurtosis of surface texture height distribution	$S_{ku} = \frac{1}{MN S_q^4} \sum_{j=1}^N \sum_{i=1}^M z^4(x_i, y_j)$
$S_{al}$	Fastest decay autocorrelation length	$S_{al} = \min(\sqrt{\tau_x^2 + \tau_y^2})$ with $\tilde{R}(\tau_x, \tau_y) \leq 0.2$
$S_{dr}$	Developed interfacial area ratio	$S_{dr} = \frac{\sum_{j=1}^{N-1} \sum_{i=1}^{M-1} A_{i,j} - (M-1)(N-1)\Delta x \Delta y}{(M-1)(N-1)\Delta x \Delta y} \cdot 100\%$
$S_{ci}$	Core fluid retention index	$S_{ci} = \frac{V_c}{S_q} = \left[ \frac{V_c(h_{0.05}) - V_c(h_{0.95})}{(M-1)(N-1)\Delta x \Delta y} \right] / S_q$
$S_{vi}$	Valley fluid retention index	$S_{vi} = \frac{V_v}{S_q} = \left[ \frac{V_v(h_{0.95})}{(M-1)(N-1)\Delta x \Delta y} \right] / S_q$

**Table 4**  
The nominal composition of GH4169 superalloy (wt. %).

<b>C</b>	<b>Cr</b>	<b>Ni</b>	<b>Co</b>	<b>Mo</b>	<b>Al</b>	<b>Ti</b>	<b>Nb</b>	<b>Fe</b>
≤ 0.08	17–21	50–55	≤ 1	2.8–3.3	0.2–0.6	0.65–1.25	4.75–5.5	Balance
<b>Mn</b>	<b>B</b>	<b>Mg</b>	<b>Si</b>	<b>P</b>	<b>S</b>	<b>Cu</b>	<b>Ca</b>	<b>Pb</b>
<0.35	<0.006	<0.01	<0.35	<0.015	<0.015	<0.30	<0.01	0.0005

**Table 5**  
The physical and mechanical properties of GH4169.

$T$ (°C)	Yield strength $\sigma_{0.2}$ (MPa)	Tensile strength $\sigma_b$ (MPa)	Elongation d $\delta_5$ (%)	Thermal conductivity (W/(m °C))	Modulus of elasticity, $E$ (GPa)	Melting point (°C)	Hardness (HV)	Density (g/cm <sup>3</sup> )
20	1240	1450	>10	13.4	205	1310	376–480	8.24
650	1000	1170	>12	22.1	205	—	—	—
750	740	950	25	23.5	—	—	—	—

of the surface, is an extension of 2D surface roughness parameter  $R_a$ . Their discrete forms, along with other 3D surface texture parameters, are listed in the Table 3. For these equations,  $z(x_i, y_j)$  is the height of sampling point  $(x_i, y_j)$  on  $X$ – $Y$  plane;  $M$  is the number of sampling points in  $X$  direction;  $N$  is the number of sampling points in  $Y$  direction.

### 3. Materials and methods

It is commonly accepted that micro geometrical features and corresponding texture parameters of a machined surface mainly depends on the selected machining processes and material properties [28–30]. Variations in these features can now be accurately analyzed and investigated by using 3D surface texture characterization techniques. In this research, by comparing and analyzing the experimentally-measured 3D surface texture parameters and corresponding geometrical features, a practical correlation between the surface micro geometrical features and characterization parameters with the functionality-related performance is established for the turned and the ground surfaces.

#### 3.1. Workpiece material

For the machining experiments, a difficult-to-machine material, Ni-based superalloy GH4169, was used as workpiece material. GH4169 is of good heat resistance, high-temperature strength and corrosion resistance. Its nominal composition and physical properties of the workpiece material are given in Tables 4 and 5, respectively.

The geometry of the workpieces for both grinding and turning experiments were supplied in the form of bar, 30 mm diameter and 100 mm length, as shown in Fig. 5.

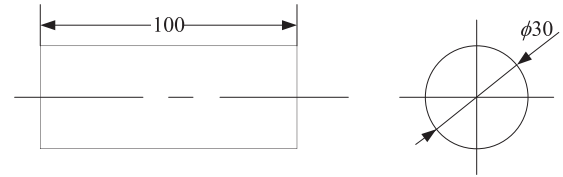


**Fig. 5.** Experimental workpiece shape and size.

#### 3.2. Experimental method

External plunge grinding and external cylindrical turning experiment were carried out separately with different processing parameters. The grinding wheel adopted is monocrystalline fused alumina (SA80) and its abrasive grit size is 80#. External turning was carried out with Sandvik GC1105 tool insert with a TiAlN coating. Details of cutting tools and experimental conditions are given in Table 6.

#### 3.3. Measurements and analyses

After the grinding and turning experiments, surface topographical characteristics and surface texture parameters for the workpiece were measured, compared by means of SEM and white light interferometry which has nano-scale resolution on its optical  $Z$ -axis. The ground and turned surfaces generated are of identical values of 3D arithmetic mean deviation ( $S_{a,grinding} = S_{a,turning} = 0.30 \mu\text{m}$ ). Statistical functions (e.g. PSD and ACV) and 3D surface texture parameters were detailedly analyzed. Other functional properties of the ground and turned surfaces were correlated and assessed using the 3D surface texture parameters and appropriate statistical functions.



**Table 6**

Machining processing parameters and tool properties for grinding and turning experiments.

Machining parameters			Tool/insert/coating material		Surface texture parameter(s)
Grinding	Wheel speed	Workpiece speed	Depth of cut	Monocrystalline fused alumina (SA80), grit size 80# Sandvik GC1105 (TiAlN coating)	$S_{a,grinding} = 0.30 \mu\text{m}$
	$v_s = 25 \text{ m/s}$	$v_w = 16 \text{ m/min}$	$a_p = 0.02 \text{ mm}$		
Turning	Cutting speed	Feedrate	Depth of cut	Sandvik GC1105 (TiAlN coating)	$S_{a,turning} = 0.30 \mu\text{m}$
	$v = 95 \text{ m/min}$	$f_r = 0.1 \text{ mm/r}$	$a_p = 0.1 \text{ mm}$		

**Table 7**

Surface characterization parameters for the ground and turned surfaces.

2D parameters	Ground	Turned	3D parameters	Ground	Turned	Statistic functions	Ground	Turned
$R_a (\mu\text{m})$	0.30	0.30	$S_a (\mu\text{m})$	0.30	0.30	ADF	Fig. 8(a)	Fig. 8(a)
$R_q (\mu\text{m})$	0.38	0.36	$S_q (\mu\text{m})$	0.38	0.36	BAC	Fig. 8(b)	Fig. 8(b)
$R_t (\mu\text{m})$	3.28	2.33	$S_{sk}$	−0.05	0.04	PSD	Fig. 9(b) and (c)	Fig. 9(e) and (f)
$R_{sk}$	−0.05	0.04	$S_{ku}$	3.18	2.35	ACV	Fig. 10(a) and (b)	Fig. 10(c) and (d)
$R_{ku}$	3.18	2.35	$S_{al} (\mu\text{m})$	3.28	11.97			
$R_k (\mu\text{m})$	0.92	1.03	$S_{\Delta q} (\text{deg})$	28	9.16			
$R_{pk} (\mu\text{m})$	0.41	0.25	$S_{dr}$	12.45	1.28			
$R_{vk} (\mu\text{m})$	0.42	0.22	$S_{bi}$	0.59	0.62			
$Mr1$	12%	8.23%	$S_{ci}$	1.59	1.51			
$Mr2$	89.49%	91.61%						

## 4. Results and discussion

### 4.1. Evaluation and correlation of surface characterization parameters with functionalities

For accurate analysis and further correlation, the measured 2D/3D surface parameters and statistical functions for describing, correlating and evaluating the micro geometrical features with functionality-related properties of the ground and turned surfaces are given in Table 7.

The measured arithmetic mean deviations for the ground and turned surfaces ( $R_{a,grinding} = R_{a,turning} = 0.30 \mu\text{m}$ ) are identical. Their measured root-mean-square deviations are also with close values ( $R_{q,grinding} = 0.38$ ;  $R_{q,turning} = 0.36 \mu\text{m}$ ). If only these two surface roughness parameters were adopted to evaluate and characterize the machined surfaces, it will be easily find that they are not comprehensive enough to differentiate these two surfaces in geometry and in potential surface performance. So, more 3D surface parameters and statistic functions are introduced.

As mentioned in Table 3,  $S_{sk}$  is the measure of asymmetry of surface deviations about the mean plane. Like its 2D counterpart  $R_{sk}$ , this parameter can be used effectively to describe the shape of surface texture height distribution. For a surface which meets Gaussian distribution and has a symmetrical shape of surface height distribution, its  $S_{sk}$  equals to 0. This parameter could give some indication of the existence of spike-like features on the surface. The negative value of skewness ( $S_{sk,grinding} = -0.05$ ) indicates a slight predominance of rounded peaks and sharp valleys for the ground surface; while the positive value of skewness ( $S_{sk,turning} = 0.04$ ) means comparatively more sharp peaks and rounded valleys for the turned surface.

$S_{ku}$  is the measure of peakedness of the surface height distribution and it characterizes the spread of the height distribution. For a surface which meets Gaussian distribution, its  $S_{ku}$  equals 3; for a centrally-distributed surface, normally its  $S_{ku}$  is larger than 3; whereas for a surface meeting well-spread height distribution, its  $S_{ku}$  is smaller than 3. The measured value of kurtosis for the ground surface ( $S_{ku,grinding} = 3.18 > 3$ ) indicates that the surface texture height is slightly leptokurtically distributed and congregates near the mean line with an occasional high peak or deep valley; while for the turned surface with  $S_{ku,turning} = 2.35 < 3$ , the surface texture is platykurtically distributed and more surface height congregates at the two extremes of surface height.

$S_{al}$ , the fastest decay autocorrelation length, is a parameter in length direction and used to describe the autocorrelation characteristic of the

areal auto-correlation function (AACF). It is defined as the horizontal distance of the AACF at which it has the fastest speed to decay to its 20%. For an anisotropic surface,  $S_{al}$  is in the direction perpendicular to the surface lay. A large value of  $S_{al}$  normally denotes that the surface is dominated by low frequency (or long wavelength) components. The large value of fastest decay autocorrelation length for the turned surface ( $S_{al,turning} = 11.97 > S_{al,grinding} = 3.28$ ) means that the turned surface is more anisotropic and has dominant low frequency surface texture component which is vertical to the machining direction, as seen in Figs. 6(b) and 7(b).

$S_{dr}$ , the developed interfacial area ratio, is defined as the ratio of the increment of the interfacial area of a surface over the sampling area. A large value of  $S_{dr}$  indicates the significant complexity of either the amplitude or the spacing or both. The developed interfacial area ratio for the ground surface ( $S_{dr,grinding} = 12.45$ ) is far larger than that of the turned surface, which indicates the ground surface is of significant complexity either in its horizontal and vertical directions; it has more complicated micro geometrical features than the turned surface does. The root-mean-square slope of the ground surface,  $S_{\Delta q}$ , which is 28 and around 3 times that of the turned surface, indicates the micro asperities or peaks of the ground surface tilt more severely or are sharper than that of the turned surface.

$S_{ci}$  and  $S_{vi}$  are functionality-related parameters. They are the core and valley fluid retention indexes respectively. A large value of  $S_{ci}$  or  $S_{vi}$  indicates good fluid retention in the core zone or the valley zone of the machined surfaces. For a Gaussian surface, the  $S_{ci}$  is normally 1.56. In experiment, the core fluid retention  $S_{ci}$  and valley fluid retention  $S_{vi}$  of the ground surface (1.59 and 0.11) are slightly larger than those of the turned surface (1.51 and 0.09), which indicates the ground surfaces could retain fluids, such as lubricants, more effectively than the turned surfaces.

With a complementary use and comparison of the above-mentioned 3D surface parameters, it is possible to differentiate the ground and turned surfaces more specifically. These micro-geometry-based parameters also provide a direct means to evaluate and correlate with the functionality-related performance, e.g. surface lubricant retention ability, friction and abrasion, load bearing capability of the surface asperity

### 4.2. Evaluation and correlation and effect of statistical functions

#### 4.2.1. ADF and BAC analyses of the ground and turned surfaces

Photographs of the overall topography and texture of the ground and turned surfaces are shown in Fig. 6. Both surfaces have the same value of

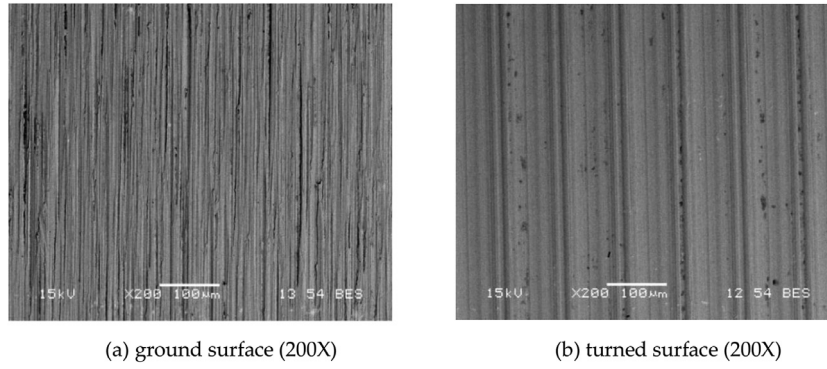


Fig. 6. SEM of surface texture for ground and turning surfaces ( $S_{a, \text{grinding}} = S_{a, \text{turning}} = 0.30 \mu\text{m}$ ).

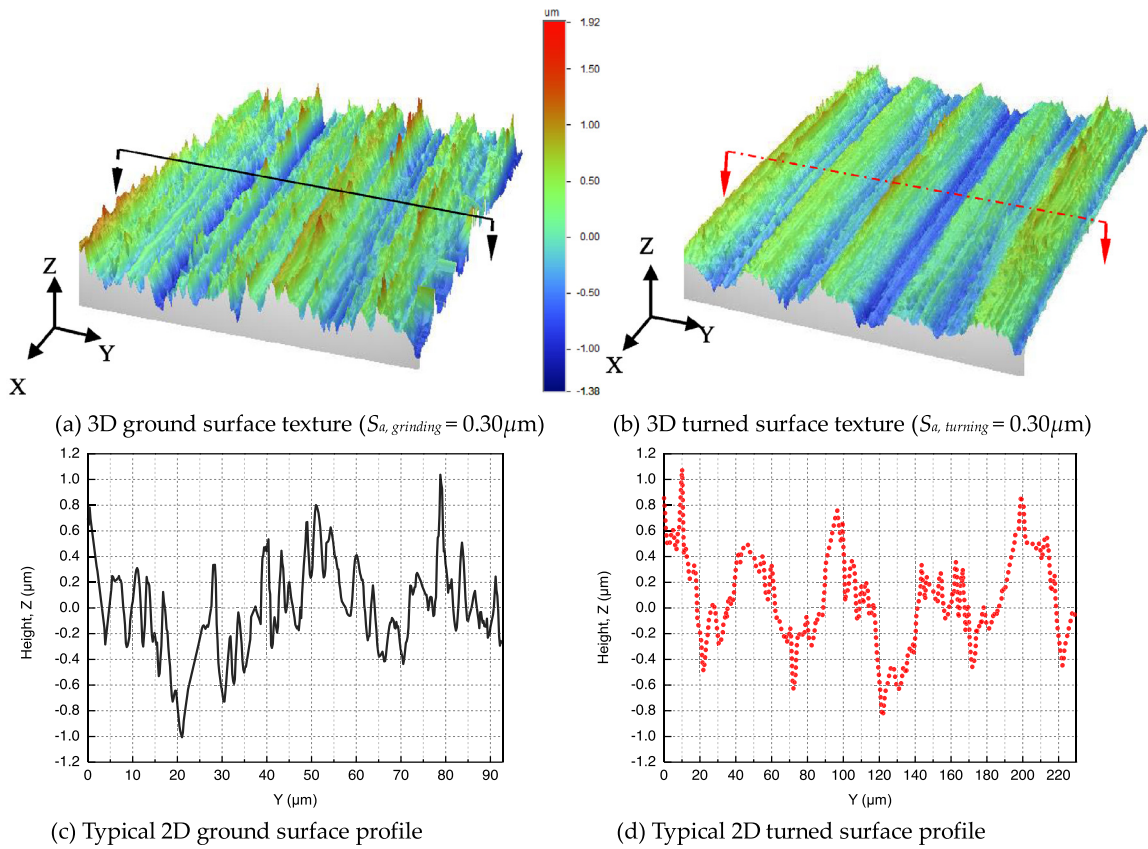


Fig. 7. 3D surface texture and 2D surface profiles of the ground and turned surfaces.

3D arithmetic mean deviation, i.e.  $S_{a, \text{grinding}} = S_{a, \text{turning}} = 0.30 \mu\text{m}$ . However, in Fig. 6 it can be clearly seen that the two surfaces differ significantly both in their appearance and micro geometrical structure, which probably results in different functionalities in corresponding applications. The ground surface does not contain distinct or regular spacing between the scratch marks. The spacings are in a range from very small to about ten microns. But, for the turned surface, obvious lays and regular grooves induced by the turning tool are left; these equal-interval grooves are very likely to be relevant to the geometry of the turning tool tip and the feed rate of turning process. For better visualization of the machined surfaces, 3D surface texture with enriched geometrical structure and colored height distribution for the ground and turned surfaces are presented in Fig. 7(a) and (c). Fig. 7(b) and (d) gives the extracted 2D surface profiles of the ground and turned surfaces respectively. Similar to the SEM photographs in Fig. 6, the surface topography of the ground surface is more random in micro geometrical structure though

its shallow scratches are generally parallel to each other; while the turned surface consists of approximately regular and parallel grooves. It is noted that only a small area could be scanned on X–Y plane of the machined surface with the white light interferometry. The scanned areas are  $121.9 \times 92.7 \mu\text{m}$  for ground surface and  $302.1 \times 229.8 \mu\text{m}$  for turned surface.

Although the values of  $S_a$  for the two machined surfaces were the same, their geometrical textures and corresponding ADFs and BACs were very different, as shown in Fig. 8; their surface texture characterization parameters (in Table 7) reflect different functional performances, such as load-bearing capability and bedding rate during running-in situation. As shown in Fig. 8(a), the ADF curve of the ground surface is much closer to Gaussian distribution than that of the turned surface. This means the ground surface has a more random surface texture (micro geometrical features) and the turned surface is comparatively texture-anisotropic. The ADF curve of turned surface is slightly

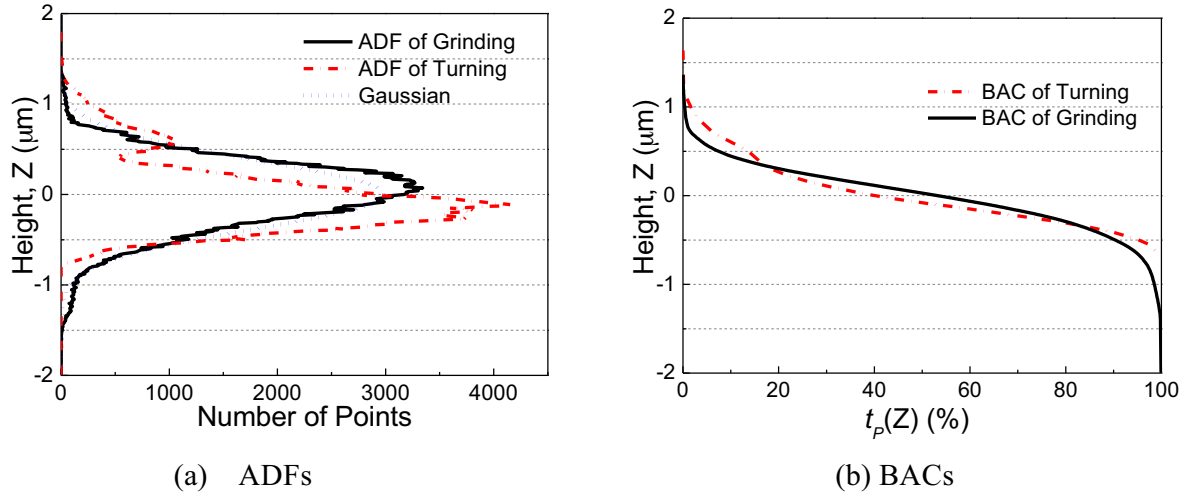


Fig. 8. Comparisons of ADF and BAC curves between the ground and turned surfaces.

negatively deviated from Gaussian distribution which means the turned surface is of higher probability density near the surface height zone below the mean line. As shown in Fig. 8(b), the BACs of the ground surface and the turned surface are also given differently though the 2 surfaces have the same  $S_a$  value. Due to the sharper gradient at the beginning of its BAC, the ground surface exhibits a quicker running-in stage when compared with that of the turned surface if contact or friction loading is applied on the surfaces; besides, larger reduced peak height ( $R_{pk, grinding} = 0.41 \mu m > R_{pk, turning} = 0.25 \mu m$ ) and peak material portion ( $M_{r1, grinding} = 12\% > M_{r1, turning} = 8.23\%$ ) means the ground surface has more material joined in the contact or been worn out, which indicates better load-bearing ability. Comparatively larger reduced valley depth ( $R_{vk, grinding} = 0.42 \mu m$ ) and the sharper gradient of the BAC at the end, the ground surface shows better lubricant or oil retention capability than that of the turned surface.

#### 4.2.2. PSD and ACV analyses of the ground and turned surfaces

The random nature of the 3D surface texture/topography of ground and turned surfaces was analyzed using the statistical functions PSD and ACV. Based on Fourier analysis, surface texture is assumed to be composed of a series of sine waves with different frequencies and amplitudes and the power spectral density function (PSD) is considered a measure of the amplitude of each harmonic component for a specific frequency and along a given direction. Thus, for 3D surface texture, the PSD plot appears as color-scaled function values upon an  $X$ - $Y$  plane. The magnitude of PSD (displayed on the  $Z$  axis) represents the amplitude of the sine wave at a specific spatial frequency for a given direction. Besides, it could average all  $X$  or  $Y$  profiles' PSD to get the values of PSD along only the  $X$  or  $Y$  axial direction.

Fig. 9 illustrates the measured 3D surface textures and related statistical function curves of the ground and turned surfaces by using a 3D optical interferometer. Identical to Fig. 7(a) and (b), Fig. 9(a) shows shallow scratches along the grinding direction  $X$  on the ground surface; while in Fig. 9(d), obvious lays and regular grooves parallel to the turning direction  $X$ , which form periodic peaks and valleys along the  $Y$  axis. Fig. 9(b) shows the magnitude of PSD plotted with the color scale over the ground surface; its average PSD curve along the  $Y$  direction, as shown in Fig. 9(c), fluctuates with respect to the spatial frequency and finally falls to zero. A dozen of spikes in the curve indicate that there are high-frequency harmonic components along the  $Y$  direction and these overlapping harmonics of various frequencies complicate the surface texture. This could be caused by the irregular nature of the abrasive grains in the grinding wheel. Fig. 9(e) shows that the magnitude of PSD over the turned surface is generally much larger than that of ground surface, though the two surfaces have the same  $S_a$  value. Fig. 9(f) shows

the average PSD along the  $Y$  direction having a dominant spatial frequency ( $f = 20 \text{ mm}^{-1}$ ), which means the turned surface has a kind of periodic geometrical structure (sinusoidal) and the magnitude of the spatial frequency is redeemed to be closely correlated with the feed rate of the turning process and tip radius of cutting tool.

By contrast, the average PSD along  $Y$  for the ground surface, shown in Fig. 9(c), has an overall trend of monotonic descent but with more randomized micro geometrical features when compared with that of the turned surface. From Fig. 9(b), (c), (e) and (f), it can be seen that PSD characteristics differ greatly between ground and turned surfaces; it reflects that PSD could be a sensitive characteristic to differentiate typical surfaces produced by different machining processes.

Another means to look into the surface information is to take the inverse Fourier transform of PSD and derive its ACV. The ACV is useful for visualizing the correlative degree of periodicity and the randomness of a surface. The contour plots of ACV normally presents the straightforward surface patterns in terms of color scale. For a random 2D surface profile, its ACV normally decays quickly in the vicinity of zero; but if the surface has a steady periodic component, the ACV will oscillate accordingly. The spacing, over which the ACV oscillates, is usually termed 'repeatability length'. The repeatability length is normally related to the machining process adopted, such as feed rate of turning.

Fig. 10(a) and (c) directly shows the periodic difference in the ACVs over the ground and turned surfaces. Fig. 10(a) depicts the ACV contour plot over the ground surfaces with color scale; and as shown in Fig. 10(b), its ACV along  $Y$  direction rapidly falls to zero from the middle of the scanned ground surface. The ground surface exhibits a fast decaying ACV with only a small magnitude of periodic oscillation. This means the ground surface is topographically more random than that of the turned surface, though both surfaces have the same 3D surface arithmetic mean roughness ( $S_{a, grinding} = S_{a, turning} = 0.30 \mu m$ ). Fig. 10(c) shows the contour magnitude of ACV over the turned surface for which periodic stripe patterns are obvious; its ACV along the  $Y$  direction, as shown in Fig. 10(d), oscillates with comparatively regular and consistent value of amplitude. This means the periodicity of surface micro geometry for the turned surface is much stronger than that for the ground surface. All of these features indicate that the turned surface is typically anisotropic and of dominant periodic wavelength structure when compared with the ground surfaces.

## 5. Conclusions

Surface texture characterization plays a vital part in describing surface micro geometrical features and in determining surface functionality-related properties (such as load bearing capacity, friction,



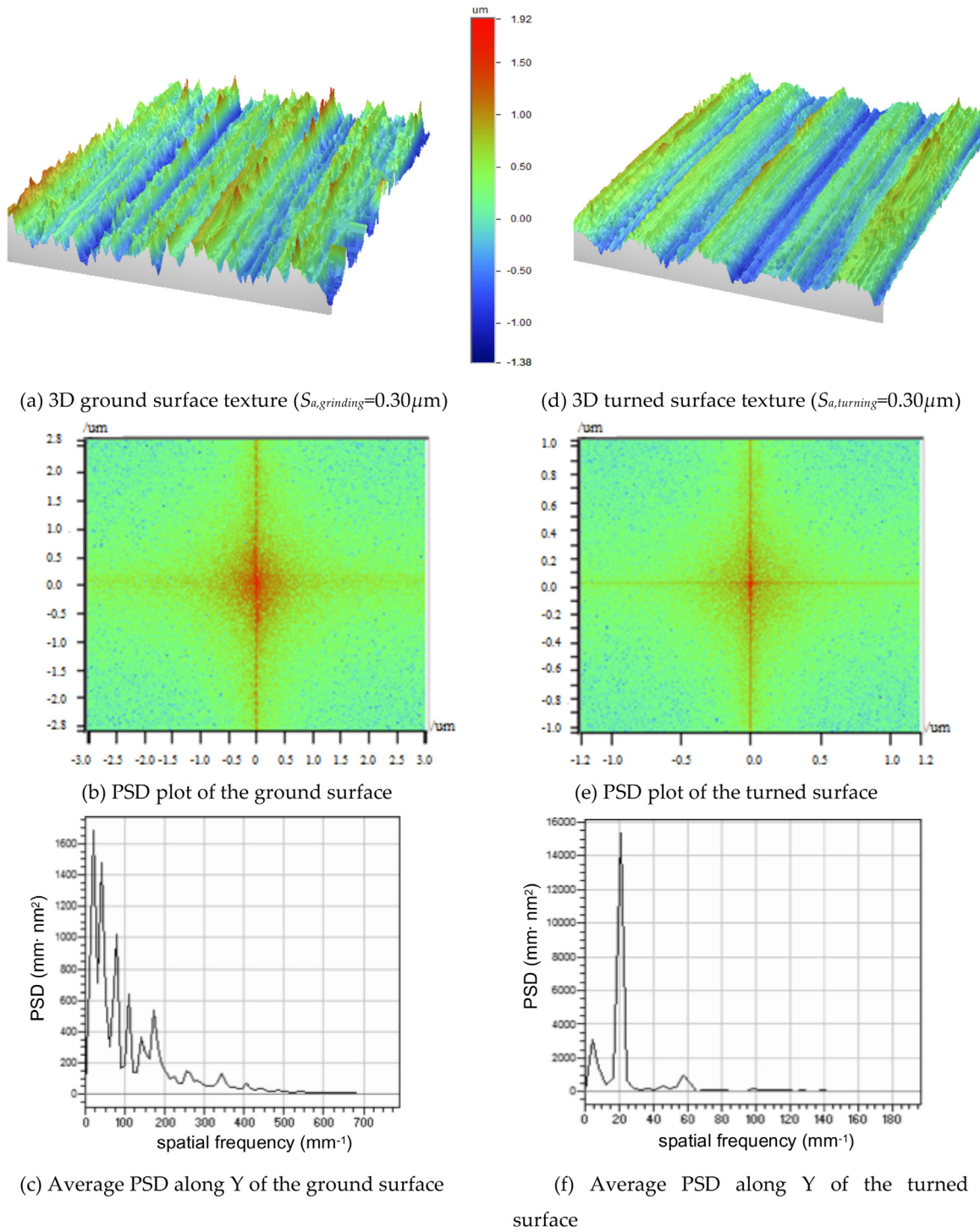


Fig. 9. Comparison of surface texture and PSDs for ground and turned surfaces ( $S_{a,grinding} = S_{a,turning} = 0.30 \mu m$ ).

wear and fluid retention capability) of machined components. Selecting reasonable surface texture characteristic parameters and correlating them with corresponding functionalities for specific engineering applications are critical for effective characterization and assessment of the quality of machined surfaces. The work and the results reported in this paper introduced a practical and effective means to implement accurate characterization and correlation. The following conclusions may be drawn from the work carried out:

- 1 Although both the ground and turned surfaces had the same value of the principal index  $S_a$ , their surface micro geometrical features

differ greatly indicating totally distinct performance properties. Apparently, it is insufficient to rely on only one or several single-valued principal surface parameters when a comprehensive characterization or assessment of the surface micro geometry and functionality are required.

- 2 When compared with the 2D or 3D single-valued surface texture parameters, statistical functions could give more information which sometimes indicates a particular functional property of machined surfaces. For the 2 experimentally-machined surfaces of Ni-based superalloy GH4169, ADFs and BACs demonstrated better load-bearing

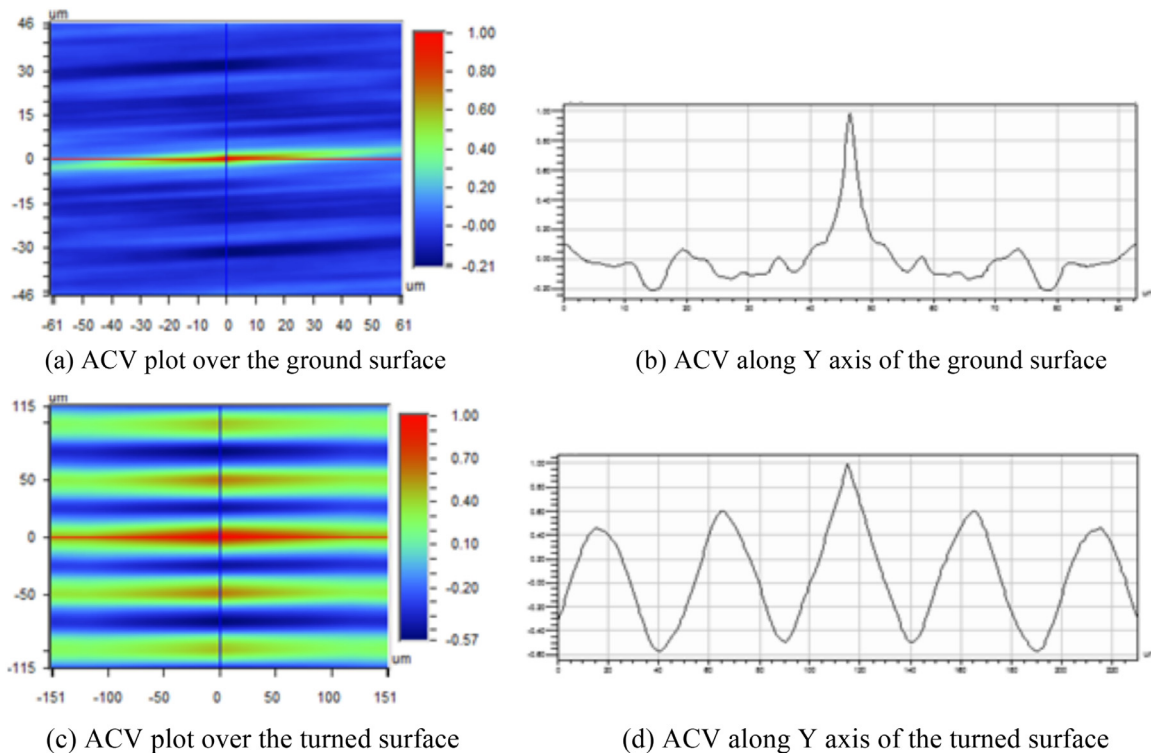


Fig. 10. Comparison of ACV plots for the ground and turned surfaces ( $S_{a, \text{grinding}} = S_{a, \text{turning}} = 0.30 \mu\text{m}$ ).

and oil retention abilities of the ground surface than those of the turned surface; while PSD and ACV gave the straightforward comparison of the randomness or periodicity of the ground and turned surface patterns.

- 3 Reasonable selection and use of 3D surface texture characterization with statistical functions (e.g. ADFs and BACs), could give more specific and complete descriptions and evaluation of the micro geometry and functionality-related properties for the machined surfaces that having the identical values in their principal indexes, such as  $S_a$  or  $R_a$ .
- 4 Effective characterizing and correlating the surface texture parameters or statistical functions with specific functionality-related properties is necessary and viable in practical production. 3D surface texture parameters and statistical functions are superior in characterizing and evaluating surface quality and corresponding functionality-related performance of machined components, when compared with the traditional situation which only using single-valued surface parameters.

## Acknowledgments

The authors would like to thank UK EPSRC for their support to the reported work undertaken through funding the “Micro-3D” project (EP/K018345/1).

## References

- [1] Sedlaček M, Podgornik B, Ramalho A, Česnik D. Influence of geometry and the sequence of surface texturing process on tribological properties. *Tribol Int* 2017;115:268–73. <https://doi.org/10.1016/j.triboint.2017.06.001>.
- [2] Zhou Y, Zhu H, Zhang W, Zuo X, Li Y, Yang J. Influence of surface roughness on the friction property of textured surface. *Adv Mech Eng* 2015;7(2):1–9. <https://doi.org/10.1177/1687814014568500>.
- [3] Cui S, Gu L, Fillon M, Wang L, Zhang C. The effects of surface roughness on the transient characteristics of hydrodynamic cylindrical bearings during startup. *Tribol Int* 2018;128:421–8. <https://doi.org/10.1016/j.triboint.2018.06.010>.
- [4] Tang Z, Liu X, Liu K. Effect of surface texture on the frictional properties of grease lubricated spherical plain bearings under reciprocating swing conditions. *Proc Inst Mech Eng Part J J Eng Tribol* 2016;231(1):125–35.
- [5] Sedlaček M, Podgornik B, Česnik D. Influence of surface texturing sequence on fatigue life and tribological properties of coated tool steel. *Key Eng Mater* 2018;767:85–92. <https://doi.org/10.4028/www.scientific.net/KEM.767.85>.
- [6] Fashina AA, Adama KK, Oyewole OK, Anye VC, Asare J, Zebaze Kana MG, Soboyejo WO. Surface texture and optical properties of crystalline silicon substrates. *J Renew Sustainable Energy* 2015;7:063119. <https://doi.org/10.1063/1.4937117>.
- [7] He CL, Zong WJ, Zhang JJ. Influencing factors and theoretical modeling methods of surface roughness in turning process: state-of-the-art. *Int J Mach Tools Manuf* 2018;129:15–26. <https://doi.org/10.1016/j.ijmachtools.2018.02.001>.
- [8] DeChiffre L, Lonardo PM, Trumpold H, Lucca DA, Goch G, Brown CA, Raja J, Hansen HN. Quantitative characterisation of surface texture (keynote paper). *CIRP Ann Manuf Technol* 2000;49(2):635–42.
- [9] Griffiths BJ. Manufacturing surface technology – surface integrity and functional performance. London, UK: Penton Press; 2001. ISBN 1-8571-8029-1.
- [10] Quinsat Y, Lavernhe S, Lartigue C. Characterization of 3D surface topography in 5-axis milling. *Wear* 2011;271(3–4):590–5.
- [11] Samuel GL. Measurement systems for characterisation of micro/nano-finished surfaces. In: Jain VK, editor. Nanofinishing science and technology – basic and advanced finishing and polishing processes. Florida, USA: CRC Press; 2017. p. 449–74.
- [12] Das J, Linke B. Evaluation and systematic selection of significant multi-scale surface roughness parameters (SRPs) as process monitoring index. *J Mater Process Technol* 2017;244:157–65.
- [13] Zheng W, Zhou M, Zhou L. Influence of process parameters on surface topography in ultrasonic vibration-assisted end grinding of SiCp/Al composites. *Int J Adv Manuf Technol* 2017;91(5–8):2347–58.
- [14] Lonardo PM, Lucca DA, DeChiffre L. Emerging trends in surface metrology. *CIRP Ann Manuf Technol* 2002;51(2):701–23.
- [15] Peters J, Bryan JB, Estler WT, Evans C, Kunzmann H, Lucca DA, Sartori S, Sato H, Thwaite EG, Vanherck P, Hocken RJ, Peklenik J, Pfeifer T, Trumpold H, Vorburger TV. Contribution of CIRP to the development of metrology and surface quality evaluation during the last fifty years. *CIRP Ann Manuf Technol* 2001;50(2):471–88.
- [16] Stout KJ, Blunt L. Three-dimensional surface topography. 2nd ed. London, UK: Penton Press; 2000. ISBN 1-8571-8026-7.
- [17] BS 1134. Assessment of surface texture – guidance and general information; 2010. ISBN 978-0-580-69913-9 p. 2010.
- [18] Blunt L, Jiang X, Stout KJ. Developments in 3D surface metrology. In: Chiles V, Jenkinson D, editors. Proceedings of the 4th international conference on laser metrology and machine performance. Southampton, UK: WIT Press; 1999. p. 255–63.
- [19] Stout KJ, Blunt L, Dong W, Mainsah E, Luo N, Mathia T, Sullivan P, Zahouani H. Development of methods for the characterisation of roughness in three dimensions. 1st ed. Oxford, UK: Butterworth-Heinemann; 2000. ISBN 9781857180237.
- [20] ISO 4287. Geometrical product specifications (GPS) – surface texture – profile method – terms, definitions and surface texture parameters; 1997. Switzerland.
- [21] ISO 13565-2. Geometrical product specifications (GPS) – surface texture – profile method – surfaces having stratified functional properties - Part 2: height characterization using the linear material ratio curve; 1996. Switzerland.

- [22] ISO 1302. Geometrical product specifications (GPS) – indication of surface texture in technical product documentation; 2002. Switzerland.
- [23] ISO 25178-2 Switzerland. accessed on 10/09/2018 <https://www.iso.org/obp/ui/#iso:std:iso:25178:-2:ed-1:v1:en>.
- [24] ISO 25178-3 Switzerland. accessed on 10/09/2018 <https://www.iso.org/obp/ui/#iso:std:iso:25178:-3:ed-1:v1:en>.
- [25] Gadelmawl ES, Koura MM, Maksou TMA, Elewa IM, Soliman HH. Roughness parameter. *J Mater Process Technol* 2002;123(1):133–45.
- [26] Taro M, Chaise T, Nélías D. A methodology to predict the roughness of shot peened surfaces. *J Mater Process Technol* 2015;217:65–76.
- [27] . Area roughness parameters accessed on 10/09/. accessed on 10/09/ <http://www.keyence.com/ss/products/microscope/roughness/surface/spk-reduced-peak-height.jsp>.
- [28] Grzesik W, Żak K. Comparison of precision hard turning and grinding operations in terms of the topographic analysis of machined surfaces. *Int J Surf Sci Eng* 2016;10(2):179–92.
- [29] Grover V, Singh AK. Modelling of surface roughness in a new magnetorheological honing process for internal finishing of cylindrical workpieces. *Int J Mech Sci* 2018;144:679–95. <https://doi.org/10.1016/j.ijmecsci.2018.05.058>.
- [30] Sedlaček M, Gregorčič P, Podgornik B. Use of the roughness parameters  $S_{sk}$  and  $S_{ku}$  to control friction – a method for designing surface texturing. *Tribol Trans* 2017;60(2):260–6.